Residual cone vision without α-transducin

Andrew Stockman Institute of Ophthalmology, University College London, London, UK

Hannah E. Smithson Department of Psychology, University of Durham, Durham, UK

Michel Michaelides Moorfields Eye Hospital, London, UK

Anthony T. Moore Moorfields Eye Hospital, London, UK

Andrew R. Webster Moorfields Eye Hospital, London, UK

Lindsay T. Sharpe Institute of Ophthalmology, University College London, London, UK

Behavioral experiments in humans with a rare genetic mutation that compromises the function of α-transducin (Gα the α-subunit of the G-protein in the primary cone phototransduction cascade) reveal a residual cone response only viable at high light levels and at low temporal frequencies. It has three characteristic properties. First, it limits temporal frequency sensitivity to the equivalent of a simple first order reaction with a time constant of approximately 140 ms. Second, it delays the visual response by an amount that is also consistent with such a reaction. Third, it causes temporal acuity to be linearly related to the logarithm of the amount of bleached pigment. We suggest that these properties are consistent with the residual function depending on a sluggishly generated cone photobleaching product, which we tentatively identify as a cone metarhodopsin. By activating the transduction cascade, this bleaching product mimics the effects of real light and is therefore one of the molecular origins of "background equivalence," the long-established observation that the aftereffects of photopigment bleaches and the effects of real background lights are equivalent. Alternative explanations for the residual cone response include the possibilities that there is a secondary phototransduction mechanism that bypasses α-transduction, or that the truncated α-transduction that results from the mutation retains some minimal functionality.

Keywords: transducin, equivalent background, photopigment bleaching, flicker sensitivity, critical flicker fusion, transduction cascade, dark adaptation

Citation: Stockman, A., Smithson, H. E., Michaelides, M., Moore, A. T., Webster, A. R., & Sharpe, L. T. (2007). Residual cone vision without α-transducin. *Journal of Vision,* 7(4):8, 1–13, http://journalofvision.org/7/4/8/, doi:10.1167/7.4.8.

Introduction

The first steps in vision occur in the rod and cone cells of the retina. Absorbed photons are converted by the G-protein-coupled phototransduction cascade into neural signals that are processed within the retina and transmitted by the optic nerves to the visual centers of the brain. α-transducin (Gα), a subunit of the heterotrimeric G-protein transducin (Gα-GDP-Gβγ), plays a crucial role in the cascade (see Figure 1 and for reviews and models, e.g., Arshavsky, Lamb, & Pugh, 2002; Hamer, Nicholas, Tranchina, Lamb, & Jarvinen, 2005; Pugh & Lamb, 2000; Pugh, Nikonov, & Lamb, 1999).

The loss of cone Gα should abolish daytime cone vision, with affected individuals becoming entirely dependent on their nighttime or rod vision (which relies on its own rod-specific Gα). However, this is not the case in a father and son, each homozygous for a frameshift mutation (M280fsX291) in the α-subunit of the cone-specific transducin (GNAT2) gene. This mutation truncates the protein sixty three amino acids prior to its carboxyl terminal (Aligianis et al., 2002), causing the loss of the important functional domains that interact with the cone opsin (Cai, Itoh, & Khorana, 2001) and with the phosphodiesterase γ-subunits (Liu, Arshavsky, & Ruoho, 1996). Surprisingly, however, both individuals retain some rudimentary cone-mediated vision (Michaelides et al., 2003).

Using tailored psychophysical procedures, we first establish that the residual daytime function in these observers is indeed cone driven, and then characterize its properties. In the absence of cone Gα, the residual function must depend on a secondary activation of the transduction cycle that somehow bypasses cone Gα. Our measurements are consistent with an activating molecule

doi: 10.1167/7.4.8 Received September 15, 2006; published March 23, 2007 ISSN 1534-7362

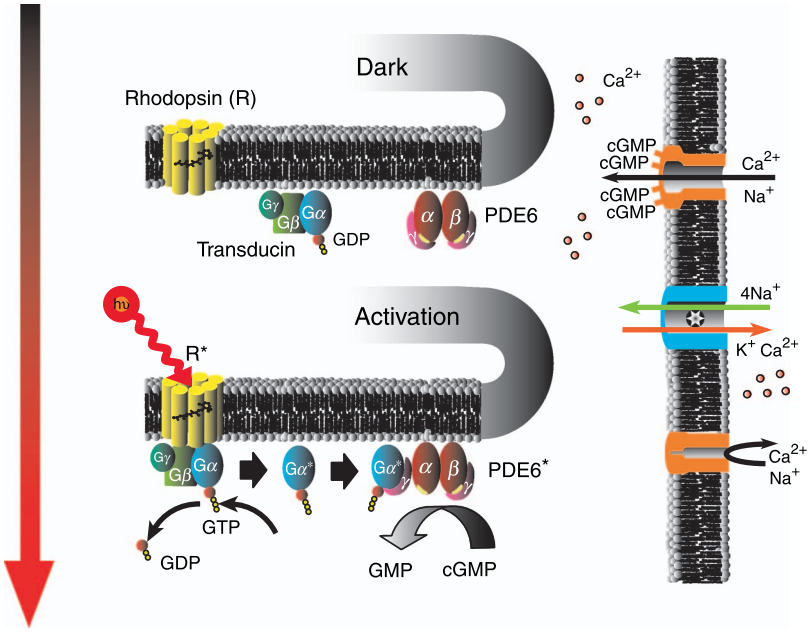

Figure 1. In the Dark (top): The chromophore molecule, 11-*cis*-retinal, lies in the pocket formed by the seven *trans*-membrane helices of the G-protein-coupled receptor protein rhodopsin (R). Both the G-protein transducin (Gα-GDP-Gβ-Gγ) and the tetrameric effector enzyme phosphodiesterase (PDE6) are in their inactive states; and the intracellular concentration of cyclic GMP is relatively high. cGMP is thus able to bind to and open cyclic-nucleotide-gated (CNG) channels in the plasma membrane, through which Ca^{2+} and Na^{+} ions flow into the cell. Activation (bottom): The absorption of a photon isomerizes the chromophore to its *all-trans* form, and triggers a conformational change of the rhodopsin into its activated state (R*). R* then activates transducin by catalyzing the exchange of GDP for GTP, which causes the separation of activated α-transducin (Gα*) from the trimer. Gα* in turn activates the phosphodiesterase enzyme (PDE6*) by exposing a site that catalyzes the hydrolysis of cGMP into GMP. The decreased cGMP concentration results in the loss of cGMP from the CNG channels, which close, blocking the inward flow of Na^{+} and Ca^{2+} ions, reducing the circulating electrical current, and hyperpolarizing the membrane voltage. Inspired by Figure 1 of Pugh et al. (1999).

that decays sluggishly with a time constant of approximately 140 ms, which we identify as a photopigment bleaching product, most likely cone metarhodopsin II (meta-II). By activating the transduction cascade, this molecule mimics the effect of real light so that it is likely to be one of the molecular origins of "background equivalence" (Stiles & Crawford, 1932); the finding that the aftereffects of photopigment bleaches are equivalent to the effects of real background lights (for reviews, see Fain, Matthews, Cornwall, & Koutalos, 2001; Lamb & Pugh, 2004; Leibrock, Reuter, & Lamb, 1998).

A particularly efficient way of scanning for cone activity is to measure temporal resolution as a function of adaptation level by determining the highest rate of flicker that can just be detected at each level. This is the temporal acuity limit or the critical fusion frequency (CFF). If a cone response is found, it can then be further characterized at frequencies below the CFF by measuring modulation sensitivity, the fraction of the light that must be flickered at constant time-averaged intensity to be just visible. Importantly, these perceptual measurements can reveal the temporal dynamics of a molecular reaction occurring within the cone photoreceptor.

Methods

Subjects

A father and son each homozygous for a frameshift mutation (M280fsX291) in the α-subunit of cone-specific transducin (GNAT2) (Michaelides et al., 2003) were the primary observers in these experiments. They are two of five members (V:7 and VI:1, respectively) of a consanguineous family diagnosed as having autosomal recessive cone dystrophy. All five have a history of nystagmus from infancy, photophobia, defective color vision, and poor visual acuity (Michaelides et al., 2003). One of the authors (AS), with normal vision, provided representative control data. After a period of training, both father and son made consistent and reproducible psychophysical settings. These studies conform to the standards set by the Declaration of Helsinki, and the procedures have been approved by local ethics committees at Moorfields Eye Hospital and at University College London.

Apparatus

Two optical systems were used for these experiments. Both were conventional Maxwellian-view optical systems

with a 2-mm entrance pupil illuminated by either a 900-W Xe arc lamp or by 75-W Xe and 100-W Hg arc lamps. Wavelengths were selected by the use of interference filters with full-width at half-maximum bandwidths of between 7 and 11 nm (Ealing or Oriel). The radiance of each beam could be controlled by the insertion of fixed neutral density filters (Oriel) or by the rotation of circular, variable neutral density filters (Rolyn Optics). Sinusoidal modulation was produced by the pulse-width modulation of fast, liquid crystal light shutters (Displaytech) at a carrier frequency of 400 Hz (which is much too fast to be resolved). The position of the observer's head was maintained by a dental wax impression. The experiments were under computer control. These systems are described in more detail elsewhere (Stockman, Plummer, & Montag, 2005).

Stimuli

The experimental conditions were chosen to favor measurements of the temporal properties of the long-wavelength-sensitive (L-) or middle-wavelength-sensitive (M-) cones. A flickering target of 4° of visual angle in diameter and either 650 or 589 nm in wavelength was presented in the center of a 9° diameter background field of 480 nm. Fixation was central. The 480-nm background, which delivered 8.26 log quanta s^{-1} deg^{-2} at the cornea, served primarily to suppress the rods (which function normally in these observers). In addition, the wavelength of the primary target (650 nm) was chosen to favor detection by cones rather than rods. The secondary target wavelength of 589 nm was used to determine the relative spectral sensitivity of the mechanism mediating flicker detection at 650 and 589 nm. As a further control to ensure that rods were not contributing to some measurements, data with the 650-nm target were replicated for the father following an intense full-field white bleach. Measurements were made during the cone plateau between 3 and 7 min following the bleach when cones have recovered but rods have not. The bleach was a white Ganzfeld (full-field) bleach of 5.42 log scotopic trolands viewed for 30 s, which bleaches approximately 60% of the rod photopigment (Pugh, 1975a). This bleach suffices to elevate rod threshold substantially during the cone plateau and for many minutes thereafter (e.g., Pugh, 1975b).

For the critical flicker fusion measurements, target radiances were varied. For the modulation sensitivity measurements, a 650-nm target was used, fixed at a time-averaged radiance of 10.38 log quanta s^{-1} deg^{-2}.

In a separate experiment to look for a short-wavelength-sensitive (S-) cone response in the affected observers, a flickering 4° target of 440 nm and variable radiance was presented in the center of a 9° background of 620 nm and 11.51 $\log_{10}$ quanta s^{-1} deg^{-2}. These conditions isolate the S-cone response in normals up to a 440-nm target radiance of about 10.5 $\log_{10}$ quanta s^{-1} deg^{-2} (e.g., Stockman, MacLeod, & DePriest, 1991; Stockman, MacLeod, & Lebrun, 1993; Stockman & Plummer, 1998). CFF measurements were made in both subjects over a range of 440 nm radiances, but no S-cone response could be measured.

The auditory stimulus for the visual–auditory phase matching experiment was produced by sending 2.5 ms square-wave pulses to a buzzer at the desired pulse rate. Thus, the "clicker" was a pulsed, broadband auditory stimulus. The visual stimuli for this experiment were the same as for the modulation sensitivity measurements, except that the modulation, in order to be visible, was set slightly suprathreshold.

Procedures

Before making any measurements, subjects light adapted to the stimuli for at least 3 min. They interacted with the computer by means of buttons and received feedback and instructions by means of tones and a computer-controlled voice synthesizer. Three types of measurements were made: (i) critical flicker fusion, in which the observers adjusted the flicker frequency (at the fixed maximum stimulus modulation of 92%) to find the frequency at which the flicker just disappeared; (ii) modulation threshold, in which the observers adjusted the flicker modulation (at a fixed frequency) to find the modulation at which the flicker just disappeared; and (iii) visual–auditory phase matching, in which auditory clicks were adjusted in phase to align perceptually with a distinct phase of the perceived flicker cycle (Stockman, Williams, & Smithson, 2004). In the last of these, the alignment setting was recorded relative to the *peak* of the perceived flicker. In practice, the subject aligned the click to the flicker iteratively using *both* the peak and the trough of the visible flicker cycle. That is, he first aligned the click with the peak, then shifted the phase of the visible flicker by 180° by pressing a button and now aligned the click with the trough, then again shifted the phase of the flicker by 180° and aligned the click with the peak, and so on. Using both phases to align the click proved more reliable than using just one. Settings could be made reliably in these experiments at frequencies up to 1 Hz.

Each data point is the average of three or four independent measurements, each of which is the average of three settings. The error bars are ±1 standard error of measurement (*SEM*).

Calibration

The radiant fluxes of test and background fields were measured at the plane of the observer's entrance pupil with a UDT Radiometer that had been calibrated by the manufacturer against a standard traceable to the National Bureau of Standards and cross-calibrated by us against our own radiometric standard (Gamma Scientific, San Diego).

Neutral density filters, fixed and variable, were calibrated in situ for all test and field wavelengths used. Interference filters were calibrated in situ with a spectroradiometer (Gamma Scientific). To convert log quanta s^{-1} deg^{-2} to log photopic trolands, subtract 7.13 from the 650-nm quantal values and 6.24 from the 589-nm quantal values. The 481-nm background of 8.26 log quanta s^{-1} deg^{-2}, which was present to suppress the rods, was 1.39 log photopic trolands or 2.53 log scotopic trolands. Target radiances are given as time-averaged values.

Results

Cone CFF versus intensity functions

Cone CFF was measured as a function of the radiance of a 650-nm target superimposed in the center of a 480-nm background of 8.26 log quanta s^{-1} deg^{-2}. Figure 2 shows the results for the affected father (gray triangles), the affected son (inverted filled triangles), and the normal control subject (open circles). With increasing target radiance, the normal cone CFF function starts to rise just above 6.5 log_{10} quanta s^{-1} deg^{-2}, and then continues to rise steadily until reaching a plateau at 43 Hz. The data for

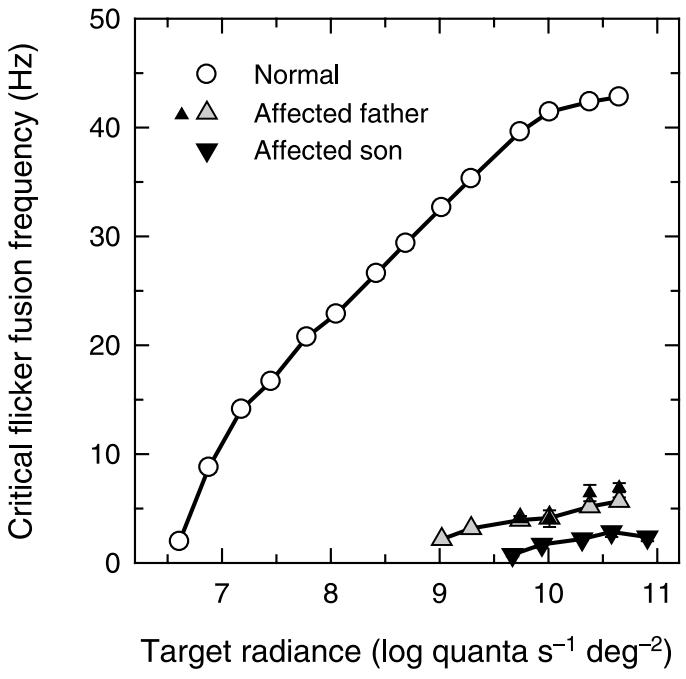

Figure 2. L-cone CFF data for the affected father (gray triangles) and son (filled inverted triangles) and for a normal observer (open circles). Measurements were made using a 650-nm target presented on a 481-nm background of 8.26 log quanta s^{-1} deg^{-2}. The small filled triangles show CFF data for the affected father measured during the rod-cone plateau following a bleach of 6.9 log scotopic trolands.

other normal observers are comparable, plateauing at frequencies ranging from 38 to 52 Hz (see also, e.g., Hecht & Shlaer, 1936; Hecht & Verrijp, 1933).

The CFF settings for the affected father and son are substantially lower than those for the normal. Flicker is first detected by the affected father at a target radiance of 9.0 log_{10} quanta s^{-1} deg^{-2} (c. 250 times higher than for the normal) and by the affected son at a radiance of 9.7 log_{10} quanta s^{-1} deg^{-2} (c. 1250 times higher). Even after the flicker becomes visible, the CFF rises to only approximately 6 Hz for the father and to only approximately 3 Hz for the son with increasing target radiance. These deficits represent a devastating loss of temporal sensitivity compared with the normal.

Although we have described the CFF functions as being cone mediated, it is crucial to confirm that this is indeed the case. Given the low CFF, it is conceivable that the flicker detection is instead being mediated by rods, perhaps through light scattered beyond the rod-saturating background. As a control, therefore, we measured the CFF in the affected father during the period following a full-field bleach of 6.9 log scotopic trolands (see Methods), when his rods are still desensitized by the bleach but normal cones have recovered (i.e., during the cone plateau). The results, which are plotted in Figure 2 as small filled black triangles, are virtually identical to the original measurements (gray triangles). We can safely conclude therefore that the CFF function in the affected father is not rod mediated.

As a further control, we measured the CFF functions in all three observers using a 589-nm target as well as the 650-nm target, so as to determine the spectral sensitivity of the photoreceptor types mediating flicker detection. The predicted 589- versus 650-nm quantal spectral sensitivity differences are 0.80, 1.56, and 2.30 log_{10} units for detection mediated by the L-, M-, and S-cones, respectively (Stockman & Sharpe, 2000), and 2.06 log_{10} units for detection mediated by the rods (based on CIE 1951 $V'(\lambda)$).

The 589 and 650 nm CFF functions are shown in Figure 3 for the affected father (top panel, triangles), the affected son (middle panel, inverted triangles), and the normal (lower panel, circles). The 589-nm data are denoted by the open symbols, and the 650-nm CFF data (replotted from Figure 2) are denoted by gray symbols. The continuous functions fitted to the 589-nm data are arbitrary, best-fitting functions generated separately for each subject by curve discovery software (TableCurve 2D, Jandel Scientific). The dashed lines are the same functions after they have been shifted horizontally along the target radiance axis to best fit the 650-nm data (using a least-squared residuals fitting criterion). As can be seen, the lateral shift accounts for the 650-nm data well, except above 40 Hz for the normal [these differences, which are likely to be due to M- and L-cone signal interactions (e.g., Stockman & Plummer, 2005a, 2005b; Stockman et al., 2005), are unimportant in this context]. The shifts are 0.86

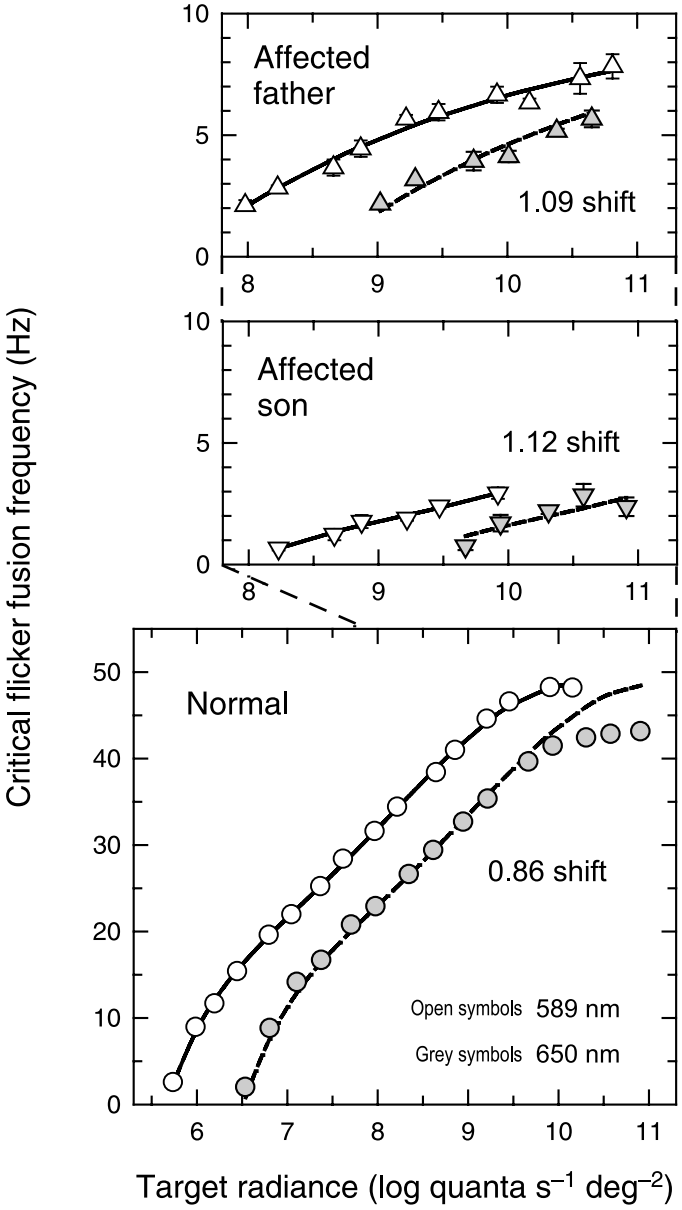

Figure 3. Cone CFF data for a normal observer (circles) and for the affected father (triangles) and son (inverted triangles). Measurements were made on a 481-nm background of 8.26 log quanta s^{-1} deg^{-2}. The grey symbols are the 650-nm target data replotted from Figure 1. The open symbols are comparable data obtained with a 589-nm target. The functions denoted by the continuous lines are arbitrary functions chosen to describe the 589-nm CFF data for each subject. The functions denoted by the dashed lines are the 589-nm functions for each subject shifted along the log radiance axis to best fit their 650-nm data. The shifts listed in the figure reflect the spectral sensitivity difference between 589 and 650 nm for the CFF measurements.

for the normal and 1.09 and 1.12, respectively, for the affected father and son. In terms of photoreceptor spectral sensitivities, the shifts are consistent with a mixed L- and M-cone detection of flicker in all subjects, with detection in the normal being more L-cone dominated than in the affected father and son. Thanks to the large discrepancies between the measured spectral sensitivity differences and the rod and S-cone predictions, we can rule out any significant involvement of those photoreceptors in the detection of 650-nm flicker. Moreover, the similarity in shape of the curve fitted to the 589-nm CFF data to that fitted to the 650-nm data, both for the father and son, is also consistent with the detection of 589 nm flicker being cone mediated. We can also exclude more exotic possibilities, such as ganglion cells containing melanopsin, because the λ_{max} of melanopsin of approximately 480 nm (see Berson, 2003) is intermediate between the rods and S-cones and would produce a much greater shift than we find.

In a series of S-cone CFF measurements over a wide range of S-cone adaptation levels, no evidence for any S-cone response could be found. It is possible that a response might be found at high S-cone bleaching levels, but such levels are considered to be potentially damaging and were not used in our experiments.

Cone modulation sensitivity functions

The CFF functions provide information about sensitivity at the temporal resolution limit, but not at lower temporal frequencies. To investigate the properties of the mechanisms mediating detection at lower temporal frequencies, we measured cone modulation sensitivities. A fixed time-averaged 650-nm radiance of 10.38 log quanta s^{-1} deg^{-2} was chosen. Like the CFF functions, the modulation sensitivities were measured on the 480-nm background.

Figure 4 shows temporal modulation sensitivities for the affected father (gray triangles), the affected son (inverted filled triangles), and the normal (open circles). The lower panel shows the data for all three observers, while the upper panel replots the data for the affected individuals at a larger scale. The data for the normal are typical for this adaptation level, peaking at approximately 7 Hz and extending to approximately 45 Hz (e.g., De Lange, 1958; Kelly, 1961). Functions like these that peak at intermediate frequencies are known as bandpass." The data for the affected individuals, as expected from the CFF measurements, are atypical. Their data extend to only 6 Hz for the father and 2 Hz for the son. In contrast to the normal bandpass sensitivity function, their sensitivity follows a "low pass" function that falls monotonically with temporal frequency. The differences between the father and son can be accounted for mainly by an overall loss of sensitivity. This is illustrated in the lower panel, in which the father's data have been vertically shifted to align with the son's data as shown by the dashed line. The best-fitting vertical shift is 0.58 log unit (i.e., a shift equivalent to an attenuation factor of 3.8).

At the lowest frequency of 0.25 Hz, the sensitivities for the affected father and son are about 3 and 10 times

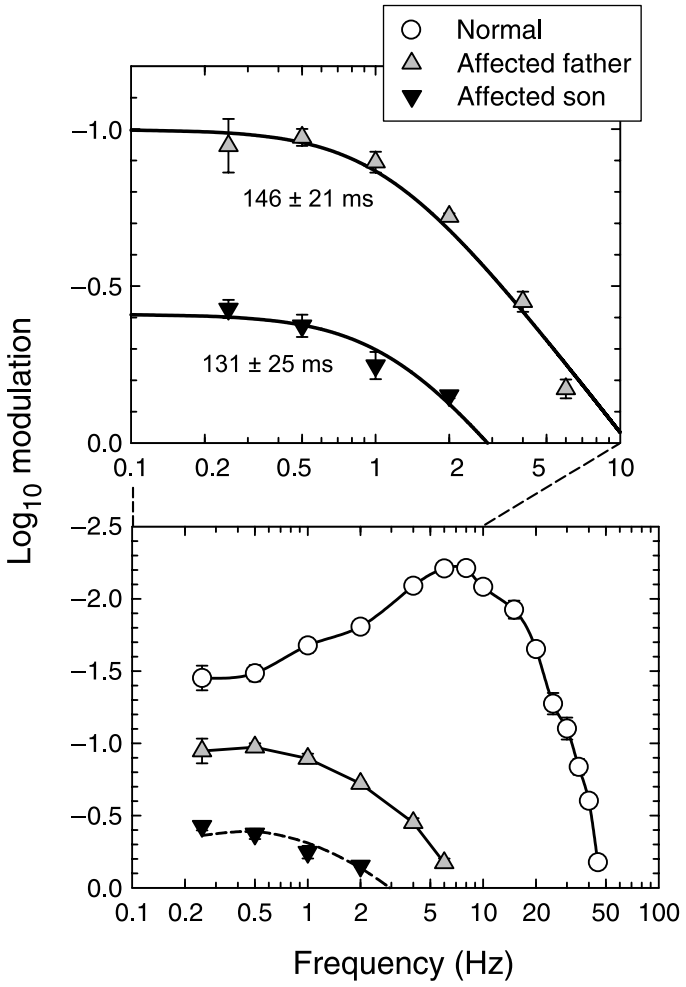

Figure 4. Cone modulation sensitivity data for a normal (circles) and for the affected father (triangles) and son (inverted triangles) measured using a modulated 650-nm target with a time-averaged radiance of 10.38 log quanta s^{-1} deg^{-2} superimposed on a 481-nm background of 8.26 log quanta s^{-1} deg^{-2}. The data for the affected observers are plotted in both panels at different scales. In the lower panel, the data for the normal and the father are connected by continuous lines. The father's data, as shown by the dashed line, have been vertically shifted by 0.58 log unit to align with the data for the son. In the upper panel, best-fitting versions of a model describing the behavior of a single leaky integrator (see Equation 1) are shown as the continuous lines. The best-fitting time constants (±1 *SE*) are noted in the panel.

lower, respectively, than that of the normal. This suggests that the father and son are able to see steady lights (0 Hz) of high radiance reasonably well. Motion or flicker that depends on temporal frequency components much above 1 or 2 Hz, however, will be largely invisible to them.

If we suppose that the temporal modulation sensitivity functions for the affected father and son depend upon light-induced changes in the amount of a particular photoproduct that activates the transduction cascade (which we shall refer to as X* for short), then the shapes of those functions should reflect the rate of production and decay of X* (in fact, they should be related to the Fourier transform of the lifetime of X*). The lifetime of X* should in turn depend on the convolution of the reaction time constants up to and including the removal of X* itself (e.g., Baylor, Hodgkin, & Lamb, 1974; Fourtes & Hodgkin, 1964). Since we are making *psychophysical* measurements, the modulation sensitivities may also reflect the temporal properties of processes in the cascade subsequent to the secondary activation by X* as well as those at postreceptoral neural stages. Potentially, then, the modulation sensitivities measured in the father and son could be complex; but, intriguingly, they are not.

We find that the modulation sensitivity data can be accounted for by a model in which the amount of the activating photoproduct, X*, is limited by a simple first-order reaction, the effect of which is comparable to that of a single leaky integrator (RC filter) with exponential decay, and with a single time constant. To evaluate this model, we fitted the standard formula for a leaky integrator (e.g., Watson, 1986) separately to the data for the father and son. The formula for the amplitude response, $A(f)$, of a single leaky integrator is

$$A(f) = \tau[(2\pi f\tau)^2 + 1]^{-0.5}, \quad (1)$$

where f is the frequency in Hertz and τ is the time constant in seconds. The fits were carried out to the logarithmic modulation thresholds as shown in Figure 3. In addition to varying τ, an additional sensitivity scaling factor (vertical logarithmic shift) was allowed. The results of the model fits, which are shown by the solid lines in the upper panel, are remarkably good with root-mean-squared errors of only 0.044 (father) and 0.031 (son) and R^2 values of 0.977 (father) and 0.915 (son). The estimated time constants (plus and minus the standard error of the fit) are 146 ± 21 ms (father) and 131 ± 25 ms (son), a similarity that suggests the kinetics of the limiting reaction are essentially the same for both observers. Different vertical shifts of −1.84 ± 0.04 for the father and −1.29 ± 0.06 for the son reflect their different sensitivities. Comparable data from normals are bandpass and are far too complex to be modelled by a single leaky integrator stage (e.g., De Lange, 1958).

The fact that the data can be accounted for by a simple first order reaction, although the amount of X* should depend on the convolution of the preceding reaction time constants, and on the time constants of later processes, suggests two things: first, that the time constant of the limiting reaction of 140 ms is much longer than those of any other relevant process; and second, that the time constants of the other stages are too short to produce any sizeable *frequency-dependent* effects on modulation sensitivity in the visible range of frequencies, which in this

case are those up to and including 6 Hz (see Figure 3). (For reference, a time constant of 20 ms would reduce the sensitivity at 6 Hz by 0.1 log unit, relative to sensitivity at 0 Hz.)

In a linear system, the order of the reactions can be changed without affecting the result (see Baylor et al., 1974, p. 702), so that we do not know where the dominant (slowest) limiting stage in the reaction cascade is with respect to X*. On the assumption that it would be inefficient to follow a slow process with a faster one, and extrapolating from the known tendency for successive steps in the retinoid cycle to become slower (Lamb & Pugh, 2004), we speculate that the most plausible limiting stage is the decay of X* itself.

Visual–auditory phase matching

Modulation sensitivity data, such as those shown in Figure 4, provide only a partial picture of the visual response. A more complete picture requires knowledge also of the visual delay. If vision is limited by a first order reaction with a time constant of approximately 140 ms, then the effects of that reaction should also be evident in the delay of the visual response. Specifically, the response of the affected subjects should be phase delayed [$P(f)$] with respect to the normal by

$$P(f) = \tan^{-1}(2\pi f\tau), \quad (2)$$

where f is the frequency in Hertz and τ is the time constant in seconds (τ = 0.146 s, for the affected father).

In psychophysics, phase delays must be measured relative to a second perceptual process. Moreover, to enable comparisons between the affected subjects and normals, that second process must be common to both groups. We therefore measured visual delays relative to an auditory reference stimulus produced by a train of clicks (clicker). Rate matching between flicker and clicker has been reported before (e.g., Bowker & Mandler, 1981; Fukuda, 1977; Gebhard & Mowbray, 1959; Shipley, 1964), but phase matching seems uncommon. In a preliminary study, we reported that phase matching in normal observers is roughly veridical at temporal frequencies below approximately 1.5 Hz but breaks down at higher frequencies, where only rate matching is possible (Stockman et al., 2004). Although limited to 1 Hz and below, the visual–auditory phase matching data reported here provide a strong test of the hypothesis that the visual response in the affected father is rate-limited by a sluggish reaction.

Figure 5 shows the visual–auditory phase delays for the normal (open circles) and the affected father (gray triangles). The visual stimuli were the same as those for the modulation sensitivity measurements shown in Figure 4, except that the flicker modulation was set to be slightly suprathreshold in order to be visible. The phase data for the normal are clearly more advanced than those for the father by up to approximately 30° by 1 Hz. When the father's data are advanced (filled triangles, dashed line) to compensate for the phase delays introduced by a leaky integrator with a time constant of 146 ms (Equation 2), the affected and normal phase data align well. We conclude therefore that both the modulation sensitivity and the phase delay data are consistent with vision in the affected observer being limited by a sluggish first order reaction.

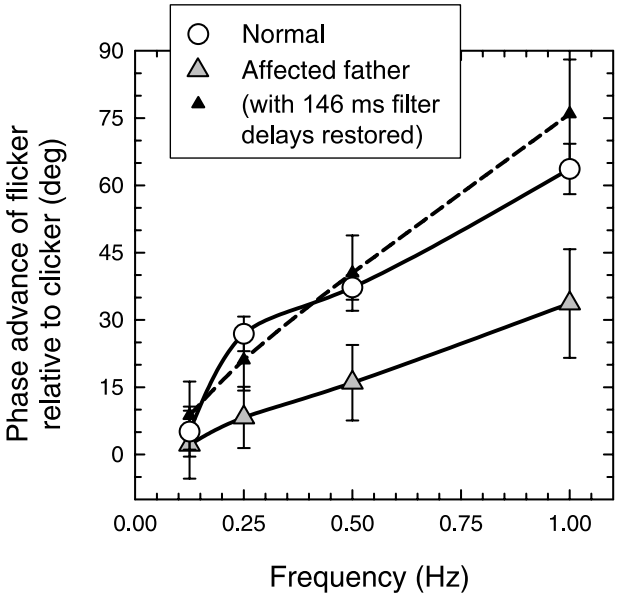

Figure 5. Phase advance of flicker needed to align peak with an auditory click for the affected father (gray diamonds) and the normal (open circles). The filled triangles show the data for the father phase advanced to compensate for the phase delays assumed to be caused by the limiting reaction. Visual stimuli as for Figure 4.

The phase measurements also provide an important control for an alternative explanation of the modulation sensitivity functions for the affected observers: that their shapes depend on an early internal noise source rather than being limited by a first order reaction. As pointed out theoretically (Graham & Hood, 1992) and shown experimentally (Rovamo, Raninen, & Donner, 1999; Rovamo, Raninen, Lukkarinen, & Donner, 1996), flicker modulation sensitivity functions measured in the presence of dominant early noise may not carry information about the shape of the underlying temporal filter. Since dominant early noise in the transduction cascade might be an indirect consequence of the Gα mutation, we were concerned that such noise may be affecting our results. However, given that any early noise should affect modulation sensitivities, but not phase delays, this alternative explanation is not supported by our combined

modulation and phase data, which show effects in both types of data that are consistent with an additional, sluggish photochemical reaction.

Discussion

Our results show that a father and son with a mutation that renders their cone Gα ineffective retain some cone-mediated visual function at high radiances, but only for stimuli of low temporal frequencies. One possibility is that this residual cone function is maintained by a secondary activation of the phototransduction cascade by a bleaching photoproduct that bypasses Gα. Two lines of evidence provide strong support for this hypothesis. First, many psychophysical and biological findings imply that bleaches produce visual signals that are equivalent to those produced by steady background lights. Such visual signals do not originate from a primary activation of the phototransduction cascade. Second, the properties of the residual cone function in our subjects are consistent with a visual process that is limited by the production of such a bleaching photoproduct, the activity of which is regulated by a reaction with a time constant of approximately 140 ms.

Equivalent background hypothesis

The equivalent background hypothesis was postulated by Stiles and Crawford (1932) as a way of accounting for the equivalence between the prolonged losses of visual sensitivity following a bleach and the losses caused by real background lights. They proposed that a hypothetical bleaching photoproduct acts like an "equivalent background" light, the intensity of which slowly fades as the photoproduct is regenerated and the system returns to its fully dark-adapted state. Although tested primarily under rod-mediated conditions (e.g., Blakemore & Rushton, 1965; Barlow & Sparrock, 1964; Crawford, 1937, 1947), this hypothesis has been found to hold approximately for cones (Geisler, 1979).

The molecular origin of the equivalent background is primarily in the photoreceptor (e.g., Graboswki & Pak, 1975; Pepperberg, Lurie, Brown, & Dowling, 1976; Weinstein, Hobson, & Dowling, 1967). The desensitization in rods following weak bleaches is due part to the activity of a metarhodopsin product, most likely MII-P-Arr (Leibrock & Lamb, 1997; Leibrock, Reuter, & Lamb, 1994; Leibrock et al., 1998), thus confirming a proposal originally made by Donner and Reuter (1967). Another photoproduct known to produce bleaching desensitization, although with lower activity, is the unregenerated "free" opsin that remains after the separation of the *all-trans*-retinoid (Cornwall & Fain, 1994; Cornwall, Matthews, Crouch, & Fain, 1995; Melia, Cowan, Angleson, & Wensel, 1997). More recently, free *all-trans*-retinal—after dissociation from rhodopsin—has been shown to inhibit the CNG channels, thus providing another route by which bleaches could mimic real light (Dean, Nguitragool, Miri, McCabe, & Zimmerman, 2002; McCabe et al., 2004). However, under physiological conditions in rod photoreceptors, this effect is extremely modest and, if similar to that in cone photoreceptors, is several orders of magnitude too slow to be mediating vision in our subjects (He et al., 2006).

The site(s) of the interaction between the bleaching products and the transduction cascade remains somewhat uncertain, although some evidence suggests that an important site is Gα itself (Matthews, Cornwall, & Fain, 1996). In our observers, however, the site of interaction cannot be cone Gα, which suggests that the photoproduct upon which their cone vision depends must interact at a site somewhere later in the cascade, such as the one where PDE6 is active, or even the CNG channels.

Further details about bleaching desensitization and dark adaptation can be found in several reviews (Fain et al., 2001; Lamb & Pugh, 2004; Leibrock et al., 1998).

Critical flicker fusion and fraction of pigment bleached

If the residual cone function in the affected father and son is correctly attributed to the activity of a bleaching product, X*, then we might expect a simple relationship to exist between their CFF and the fraction of bleached photopigment (p). In fact, we find that

$$\mathrm{CFF} = k[\log_{10}(p) + c], \tag{3}$$

where k is a constant of proportionality and c is a constant that scales p. Figure 6 shows the CFF for the father (gray triangles) and son (inverted black triangles) replotted as a function of $\log_{10}(p)$, where p was calculated using standard bleaching equations and assuming that a light of 4.3 $\log_{10}$ trolands (or 10.55 log quanta s^{-1} deg^{-2} for a 589 light) bleaches 50% of the cone pigment for prolonged (steady-state) viewing (Rushton & Henry, 1968). The 589-nm CFF data were preferred for modelling simply because they extend over a greater range of radiances. The fits of Equation 3 to each observer's data are shown by the straight lines. The parameters of the model fits are as follows: for the father $k = 2.27 \pm 0.14$ and $c = 3.60 \pm 0.15$ with an *RMS* error of 0.31 and R^2 value of 0.971; and for the son $k = 1.39 \pm 0.10$ and $c = 2.82 \pm 0.10$ with an *RMS* error of 0.10 and R^2 value of 0.981. Equation 2 is in fact a version of the Ferry–Porter law in which luminance has been replaced by p. The Ferry–Porter law, which states that CFF is linear with log radiance, is found under a variety of conditions (Ferry, 1892; Porter, 1902).

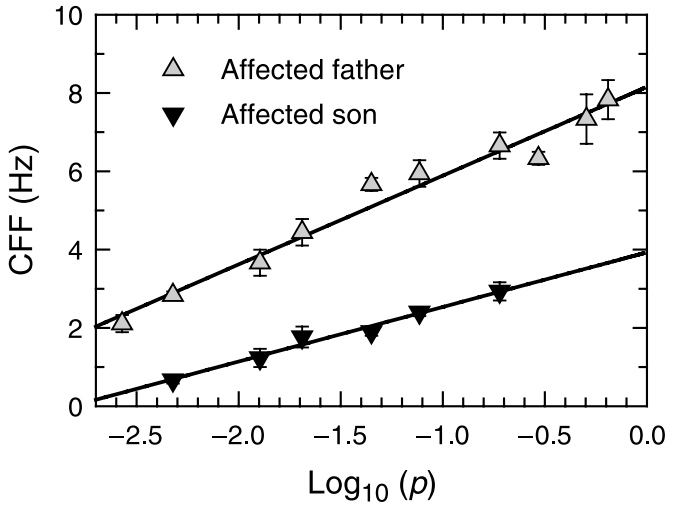

Figure 6. CFF data for the affected father (triangles) and son (inverted triangles) measured with the 589-nm target plotted as a function of the logarithm of the fraction of bleached pigment. Data replotted from Figure 2. The fraction of bleached pigment was calculated using standard bleaching equations and assuming a 50% bleach at 4.3 log trolands (Rushton & Henry, 1968). The continuous lines are best-fitting versions of Equation 3.

We note that there is not necessarily any inconsistency between Equation 3, which relates sensitivity to log(*p*), and the Dowling–Rushton equation, which relates sensitivity loss to 10^p (Dowling, 1960; Rushton, 1961). The former is assumed to depend on an early photoproduct with a time constant of decay of 140 ms, whereas the latter will also reflect the prolonged desensitization caused by more sluggishly removed photoproducts, such as the opsin.

The affected father is about 4 times more sensitive to cone stimuli than his son. We are not certain of the origin of this difference, or even whether it is receptoral or postreceptoral. Importantly, though, the inferred time constants from the modulation sensitivity measurements for the two observers are the same. Thus, although their overall sensitivities differ, the biochemical processes underlying their vision do not.

Identification of the limiting reaction

Our data suggest that the amount of X* is limited by a reaction with a time constant of approximately 140 ms that is substantially slower than other reaction steps. Given that successive steps in the retinoid cycle tend to become progressively slower (e.g., Lamb & Pugh, 2004), the time constant of 140 ms is likely to pertain to the decay of X*.

In principle, all we need do to identify X* is to find the relevant reaction in the cone retinoid cycle with a time constant close to 140 ms. In practice, however, such an identification is far from straightforward. First, most relevant data are from rods, which dark adapt more slowly than cones. Second, most photochemical data were obtained at low temperatures under physiologically unrealistic conditions, such as in detergent solution. Consequently, estimates of the time constants of decay will substantially underestimate those likely to be found in photoreceptors at body temperature. And, indeed, the available estimates of the time constants of decay of meta-II and meta-III are too slow to account for our data (see Table 1 of Imai et al., 2005).

Nonetheless, new data obtained using a fast CCD spectrophotometer with chicken green cone pigment expressed in HEK293 cells reveal a time constant of decay of meta-II of 960 ± 460 ms at 2 °C (Kuwayama, Imai, Morizumi, & Shichida, 2005). It seems plausible therefore that human cone pigment meta-II might decay with a time constant of 140 ms at 37C, since this would require less than a doubling of the reaction rate for every 10 °C rise. Therefore, we tentatively identify X* as the decay of cone meta-II by the hydrolysis of the Schiff-base bond that attaches the chromophore. However, recent microspectrophotometric measurements of meta-I and meta-II decay in single goldfish cones carried out at 20 °C can be fitted by two exponentials, of which the faster has a time constant of 5.1 s (Golobokova & Govardovski, 2006). Corrected to 37 °C, this is still slower than the rate we require to model our data.

There is relatively little psychophysical data on the dynamics of human cone dark adaptation. Perhaps the most relevant data are those of Pianta and Kalloniatis (2000), in which they identified two exponentially decaying components in the cone recovery curve: a faster component with a time constant of approximately 19 s, and a slower one with a time constant of approximately 51 s. Both of these are, however, too long to be consistent with the time constant of 140 ms inferred from the modulation sensitivity data (which is too short to have been revealed in their measurements). Pianta and Kalloniatis (2000) related their slower component to the decay of cone meta-II. Although time constants comparable to 19 s for some cone meta-II opsins are obtained using low temperature spectroscopy under nonphysiological conditions (see Table 1 of Imai et al., 2005), we believe that the decay of meta-II *in vivo* is likely to be faster.

Alternative Explanations

Although the vestigial cone-driven response is consistent with the secondary activation of the phototransduction cascade by a cone metarhodopsin photoproduct, other alternative explanations cannot be excluded. One possibility is that there is more than one cone GNAT2 gene in humans (Lerea, Bunt-Milam, & Hurley, 1989); at least one of which is spared in our subjects. Although some Southern blot analyses initially suggested that there could

be multiple GNAT2 genes (Lerea et al., 1989), more recent work is consistent with there being only a single GNAT2 gene, expressed in all cones (Morris & Fong, 1993). Moreover, a BLAST search of the GenBank, EMBL, DDBJ, and PDB sequences with the human GNAT2 coding sequence (cDNA) identified only a single gene in the human genome. Given that we find severe deficits in both affected observers under conditions that normally excite the M- and L-cones, and that we find no evidence for S-cone function at all, our data are also consistent with there being a single mutant GNAT2 gene common to all three cone types. If there is a second GNAT2 gene, which seems unlikely, then the Gα that it produces must have only a minimal and much reduced effect on vision.

Another possibility is that the truncated Gα in our subjects is not entirely dysfunctional. Although the frameshift mutation causes the loss of the important functional domains that interact with the cone opsin (Cai et al., 2001) and with the phosphodiesterase γ-subunits (Liu et al., 1996), some residual function may still remain. This possibility cannot be eliminated without a complete biochemical characterization of this frameshift mutation and its physiological consequences.

Conclusion

A mutation that should completely abolish cone vision does not. Instead, it reveals a vestigial cone-driven response that is consistent with a simple first order reaction with a time constant of approximately 140 ms. One possible explanation for this finding is that the visual response is maintained by the secondary activation of the phototransduction cascade by a cone metarhodopsin photoproduct. However, although the relationship between CFF and the amount of bleached pigment is suggestive of the involvement of a bleaching product, we cannot exclude alternative possibilities, such as that the sluggish visual response reflects a secondary phototransduction mechanism that bypasses α-transduction, or that it reflects the lifetime of the interaction between a truncated cone Gα and the activated photopigment or phosphodiesterase with very low activity.

Acknowledgments

We thank Caterina Ripamonti for experimental assistance and Rhea Eskew for comments on the manuscript. We are also grateful to Trevor Lamb for suggestions and discussions and for helping to clarify how the lifetime of a photoproduct might be related to reaction times, and to David Hunt for advice about GNAT2 coding sequences. This work was supported by the Wellcome Trust and Fight for Sight. We especially acknowledge the help of the two subjects without whom this work would not have been possible.

Commercial relationships: none.
Corresponding author: Andrew Stockman.
Email: a.stockman@ucl.ac.uk.
Address: Institute of Ophthalmology, University College London, 11-43 Bath Street, London EC1V 9EL, UK.

References

Aligianis, I. A., Forshew, T., Johnson, S., Michaelides, M., Johnson, C. A., Trembath, R. C., et al. (2002). Mapping of a novel locus for achromatopsia (ACHM4) to 1p and identification of a germline mutation in the alpha subunit of cone transducin (GNAT2). *Journal of Medical Genetics, 39,* 656–660. [PubMed] [Article]

Arshavsky, V. Y., Lamb, T. D., & Pugh, E. N., Jr. (2002). G proteins and phototransduction. *Annual review of Physiology, 64,* 153–187. [PubMed]

Barlow, H. B., & Sparrock, J. M. (1964). The role of afterimages in dark adaptation. *Science, 144,* 1309–1314. [PubMed]

Baylor, D. A., Hodgkin, A. L., & Lamb, T. D. (1974). The electrical response of turtle cones to flashes and steps of light. *Journal of Physiology, 242,* 685–727. [PubMed] [Article]

Berson, D. M. (2003). Strange vision: Ganglion cells as circadian photoreceptors. *Trends in Neurosciences, 26,* 314–320. [PubMed]

Blakemore, C. B., & Rushton, W. A. (1965). Dark adaptation and increment threshold in a rod monochromat. *Journal of Physiology, 181,* 612–628. [PubMed] [Article]

Bowker, D. O., & Mandler, M. B. (1981). Binocular flicker appears faster than monocular flicker. *Journal of the Optical Society of America, 71,* 496–498. [PubMed]

Cai, K., Itoh, Y., & Khorana, H. G. (2001). Mapping of contact sites in complex formation between transducin and light-activated rhodopsin by covalent crosslinking: Use of a photoactivatable reagent. *Proceedings of the National Academy of Sciences of the United States of America, 98,* 4877–4882. [PubMed] [Article]

Cornwall, M. C., & Fain, G. L. (1994). Bleached pigment activates transduction in isolated rods of the salamander retina. *Journal of Physiology, 480,* 261–279. [PubMed] [Article]

Cornwall, M. C., Matthews, H. R., Crouch, R. K., & Fain, G. L. (1995). Bleached pigment activates

transduction in salamander cones. *Journal of General Physiology, 106,* 543–557. [PubMed] [Article]

Crawford, B. H. (1937). The change of visual sensitivity with time. *Proceedings of the Royal Society of London, Series B: Biological Sciences, B123,* 69–89.

Crawford, B. H. (1947). Visual adaptation in relation to brief conditioning stimuli. *Proceedings of the Royal Society of London, Series B: Biological Sciences, B134,* 283–302.

De Lange, H. (1958). Research into the dynamic nature of the human fovea-cortex systems with intermittent and modulated light: I. Attenuation characteristics with white and colored light. *Journal of the Optical Society of America, 48,* 777–784. [PubMed]

Dean, D. M., Nguitragool, W., Miri, A., McCabe, S. L., & Zimmerman, A. L. (2002). *All-trans*-retinal shuts down rod cyclic nucleotide-gated ion channel: A novel role for photoreceptor retinoids in the response to bright light? *Proceedings of the National Academy of Sciences of the United States of America, 99,* 8372–8377. [PubMed] [Article]

Donner, K. O., & Reuter, T. (1967). Dark-adaptation processes in the rhodopsin rod's of the frog's retina. *Vision Research, 7,* 17–41. [PubMed]

Dowling, J. E. (1960). Chemistry of visual adaptation in the rat. *Nature, 188,* 114–118. [PubMed]

Fain, G. L., Matthews, H. R., Cornwall, M. C., & Koutalos, Y. (2001). Adaptation in vertebrate photoreceptors. *Physiological Reviews, 81,* 117–151. [PubMed] [Article]

Ferry, J. (1892). Persistence of vision. *American Journal of Science and Arts, 44,* 192–207.

Fourtes, M. G., & Hodgkin, A. L. (1964). Changes in time scale and sensitivity in the ommatidia of limulus. *Journal of Physiology, 172,* 239–263. [PubMed] [Article]

Fukuda, T. (1977). Subjective frequency in flicker perception. *Perceptual and Motor Skills, 45,* 203–210. [PubMed]

Gebhard, J. W., & Mowbray, G. H. (1959). On discriminating the rate of visual flicker and auditory flutter. *American Journal of Psychology, 72,* 521–529. [PubMed]

Geisler, W. S. (1979). Evidence for the equivalent-background hypothesis in cones. *Vision Research, 19,* 799–805. [PubMed]

Golobokova, E. Y., & Govardovskii, V. I. (2006). Late stages of visual pigment photolysis in situ: Cones vs. rods. *Vision Research, 46,* 2287–2297. [PubMed]

Graboswki, S. R., & Pak, W. L. (1975). Intracellular recordings of rod responses during dark-adaptation. *Journal of Physiology, 247,* 363–391. [PubMed] [Article]

Graham, N., & Hood, D. C. (1992). Quantal noise and decision rule in dynamic models of light adaptation. *Vision Research, 32,* 779–787. [PubMed]

Hamer, R. D., Nicholas, S. C., Tranchina, D., Lamb, T. D., & Jarvinen, J. L. (2005). Toward a unified model of vertebrate rod phototransduction. *Visual Neuroscience, 22,* 417–436. [PubMed] [Article]

He, Q., Alexeev, D., Estevez, M. E., McCabe, S. L., Calvert, P. D., Ong, D. E., et al. (2006). Cyclic nucleotide-gated ion channels in rod photoreceptors are protected from retinoid inhibition. *Journal of General Physiology, 128,* 473–485. [PubMed] [Article]

Hecht, S., & Shlaer, S. (1936). Intermittent stimulation by light: V. The relation between intensity and critical frequency for different parts of the spectrum. *Journal of General Physiology, 19,* 965–977.

Hecht, S., & Verrijp, C. D. (1933). The influence of intensity, color and retinal location on the fusion frequency of intermittent illumination. *Proceedings of the National Academy of Sciences of the United States of America, 19,* 522–535. [PubMed] [Article]

Imai, H., Kuwayama, S., Onishi, A., Morizumi, T., Chisaka, O., & Shichida, Y. (2005). Molecular properties of rod and cone visual pigments from purified chicken cone pigments to mouse rhodopsin in situ. *Photochemical & Photobiological Sciences, 4,* 667–674. [PubMed]

Kelly, D. H. (1961). Visual responses to time-dependent stimuli: I. Amplitude sensitivity measurements. *Journal of the Optical Society of America, 51,* 422–429. [PubMed]

Kuwayama, S., Imai, H., Morizumi, T., & Shichida, Y. (2005). Amino acid residues responsible for the meta-III decay rates in rod and cone visual pigments. *Biochemistry, 44,* 2208–2215. [PubMed]

Lamb, T. D., & Pugh, E. N., Jr. (2004). Dark adaptation and the retinoid cycle of vision. *Progress in Retinal and Eye Research, 23,* 307–380. [PubMed]

Leibrock, C. S., & Lamb, T. D. (1997). Effect of hydroxylamine on photon-like events during dark adaptation in toad rod photoreceptors. *Journal of Physiology, 501,* 97–109. [PubMed] [Article]

Leibrock, C. S., Reuter, T., & Lamb, T. D. (1994). Dark adaptation of toad rod photoreceptors following small bleaches. *Vision Research, 34,* 2787–2800. [PubMed]

Leibrock, C. S., Reuter, T., & Lamb, T. D. (1998). Molecular basis of dark adaptation in rod photoreceptors. *Eye, 12,* 511–520. [PubMed]

Lerea, C. L., Bunt-Milam, A. H., & Hurley, J. B. (1989). Alpha-transducin is present in blue-, green-, and red-sensitive cone photoreceptors in the human retina. *Neuron, 3,* 367–376. [PubMed]

Liu, Y., Arshavsky, V. Y., & Ruoho, A. E. (1996). Interaction sites of the COOH-terminal region of the gamma subunit of cGMP phosphodiesterase with the GTP-bound alpha subunit of transducin. *Journal of Biological Chemistry, 271,* 26900–26907. [PubMed] [Article]

Matthews, H. R., Cornwall, M. C., & Fain, G. L. (1996). Persistent activation of transducin by bleached rhodopsin in salamander rods. *Journal of General Physiology, 108,* 557–563. [PubMed] [Article]

McCabe, S. L., Pelosi, D. M., Tetreault, M., Miri, A., Nguitragool, W., Kovithvathanaphong, P., et al. (2004). *All-trans*-retinal is a closed-state inhibitor of rod cyclic nucleotide-gated ion channels. *Journal of General Physiology, 123,* 521–531. [PubMed] [Article]

Melia, T. J., Jr., Cowan, C. W., Angleson, J. K., & Wensel, T. G. (1997). A comparison of the efficiency of G protein activation by ligand-free and light-activated forms of rhodopsin. *Biophysical Journal, 73,* 3182–3191. [PubMed] [Article]

Michaelides, M., Aligianis, I. A., Holder, G. E., Simunovic, M., Mollon, J. D., Maher, E. R., et al. (2003). Cone dystrophy phenotype associated with a frameshift mutation (M280fsX291) in the alpha-subunit of cone specific transducin (GNAT2). *British Journal of Ophthalmology, 87,* 1317–1320. [PubMed] [Article]

Morris, T. A., & Fong, S. L. (1993). Characterization of the gene encoding human cone transducin alpha-subunit (GNAT2). *Genomics, 4,* 442–448. [PubMed]

Pepperberg, D. R., Lurie, M., Brown, P. K., & Dowling, J. E. (1976). Visual adaptation effects of externally applied retinal on the light-adapted isolated skate retina. *Science, 191,* 394–396. [PubMed]

Pianta, M. J., & Kalloniatis, M. (2000). Characterisation of dark adaptation in human cone pathways: An application of the equivalent background hypothesis. *Journal of Physiology, 528,* 591–608. [PubMed] [Article]

Porter, T. C. (1902). Contributions to the study of flicker: II. *Proceedings of the Royal Society of London,* A70, 313–319.

Pugh, E. N. (1975a). Rhodopsin flash photolysis in man. *Journal of Physiology, 248,* 393–412. [PubMed] [Article]

Pugh, E. N. (1975b). Rushton's Paradox: Rod dark adaptation after flash photolysis. *Journal of Physiology, 248,* 413–431. [PubMed] [Article]

Pugh, E. N., Jr., & Lamb, T. D. (2000). Phototransduction in vertebrate rods and cones: Molecular mechanisms of amplification, recovery and light adaptation. In D. G. Stavenga, W. J. de Grip, & E. N. Pugh (Eds.), *Handbook of biological physics: Vol. 3. Molecular mechanisms of visual transduction* (pp. 183–255). Amsterdam: Elsevier.

Pugh, E. N., Jr., Nikonov, S., & Lamb, T. D. (1999). Molecular mechanisms of vertebrate photoreceptor light adaptation. *Current Opinion in Neurobiology, 9,* 410–418. [PubMed]

Rovamo, J., Raninen, A., & Donner, K. (1999). The effects of temporal noise and retinal luminance on foveal flicker sensitivity. *Vision Research, 39,* 533–539. [PubMed]

Rovamo, J., Raninen, A., Lukkarinen, S., & Donner, K. (1996). Flicker sensitivity as a function of spectral density of external white temporal noise. *Vision Research, 36,* 3767–3774. [PubMed]

Rushton, W. A. (1961). Dark-adaptation and the regeneration of rhodopsin. *Journal of Physiology, 156,* 166–178. [PubMed] [Article]

Rushton, W. A., & Henry, G. H. (1968). Bleaching and regeneration of cone pigments in man. *Vision Research, 8,* 617–631. [PubMed]

Shipley, T. (1964). Auditory flutter-driving of visual flicker. *Science, 145,* 1328–1330. [PubMed]

Stiles, W. S., & Crawford, B. H. (1932). Equivalent adaptation levels in localised retinal areas. In *The Physical and Optical Societies Report* (pp. 194–211). Cambridge: Cambridge University Press.

Stockman, A., MacLeod, D. I., & DePriest, D. D. (1991). The temporal properties of the human short-wave photoreceptors and their associated pathways. *Vision Research, 31,* 189–208. [PubMed]

Stockman, A., MacLeod, D. I., & Lebrun, S. (1993). Faster than the eye can see: Blue cones respond to rapid flicker. *Journal of the Optical Society of America A, Optics and Image Science, 10,* 1396–1402. [PubMed]

Stockman, A., & Plummer, D. J. (1998). Color from invisible flicker: A failure of the Talbot–Plateau law caused by an early ehardf saturating nonlinearity used to partition the human short-wave cone pathway. *Vision Research, 38,* 3703–3728. [PubMed]

Stockman, A., & Plummer, D. J. (2005a). Long-wavelength adaptation reveals slow, spectrally-opponent inputs to the human luminance pathway. *Journal of Vision, 5*(9):5, 702–716, http://journalofvision.org/5/9/5/, doi:10.1167/5.9.5. [PubMed] [Article]

Stockman, A., & Plummer, D. J. (2005b). Spectrally-opponent inputs to the human luminance pathway: Slow +L and −M cone inputs revealed by low to moderate long-wavelength adaptation. *Journal of Physiology, 566,* 77–91. [PubMed] [Article]

Stockman, A., Plummer, D. J., & Montag, E. D. (2005). Spectrally-opponent inputs to the human luminance pathway: Slow +M and −L cone inputs revealed by intense long-wavelength adaptation. *Journal of Physiology, 566,* 61–76. [PubMed] [Article]

Stockman, A., & Sharpe, L. T. (2000). The spectral sensitivities of the middle- and long-wavelength sensitive cones derived from measurements in observers of known genotype. *Vision Research, 40,* 1711–1737. [PubMed]

Stockman, A., Williams, M. R., & Smithson, H. E. (2004). Flicker-clicker: Cross modality matching experiments [Abstract]. *Journal of Vision, 4*(11):86, 86a, http://journalofvision.org/4/11/86/, doi:10.1167/4.11.86.

Watson, A. B. (1986). Temporal sensitivity. In K. Boff, L. Kaufman, & J. Thomas (Eds.), *Handbook of perception and human performance* (vol. 1, pp. 6-1-6-43). New York: Wiley.

Weinstein, G. W., Hobson, R. R., & Dowling, J. E. (1967). Light and dark adaptation in the isolated rat retina. *Nature, 215,* 134–138. [PubMed]